Attenuation of Strain Waves in Core Samples of Three Types of Rock

Birefringent strips bonded to rock-core samples are utilized in conjunction with dynamic photoelasticity to determine attenuation coefficients, rod velocities and dynamic moduli for three rock types

by W. L. Fourney, J. W. Dally and D. C. Holloway

ABSTRACT—Dynamic photoelasticity was employed to determine the velocity of longitudinal stress waves, dynamic modulus of elasticity and attenuation coefficients in rock-core samples 1 in. (25 mm) in diameter, 18 in. (0.46 m) long. Birefringent strips bonded to the core samples of Salem limestone, Charcoal granite and Berea sandstone provided all the data needed for the dynamic characterization of these rock types.

The rods were dynamically loaded at one end with a lead-azide charge. A multiple-spark-gap camera was used to record the dynamic isochromatic-fringe patterns occurring in the birefringent strip.

Of the three rock types investigated, the Berea sandstone exhibited the largest energy losses as characterized by an attenuation coefficient of 0.0910. Salem limestone and Charcoal granite exhibited much smaller losses with attenuation coefficients of 0.0196 and 0.0024, respectively. The extremely low-energy loss associated with Charcoal granite indicates that this material transmits stress waves as well as most metals.

Introduction

One of the most undesirable effects associated with blasting in an urban environment is the damage produced on structures located adjacent to the blast site. This damage can be caused by air shock, fly rock, or ground vibrations. Proper stemming procedure and correct selection and placement of the explosive usually eliminate damage due to air shock and fly rock; however, the damage produced by ground vibrations is strongly dependent on attenuation of the strain waves transmitted through the rock media between the charge and the structure.

The purpose of this investigation was to determine attenuation coefficients for strain waves propagating in core samples taken from three types of rock—Berea standstone, Salem limestone and Charcoal granite. The method employed to observe the propagation of the strain wave down the rock core is known as the birefringent strip method which was first developed by Duffy and Lee[1] and later expanded by Frasier and Robinson.[2,3] The method involves bonding an edge of a birefringent strip to the body under investigation and viewing this sheet through a conventional polariscope. A high-speed camera or a short-duration light source is employed to record the dynamic isochromatic fringes. These patterns within the photoelastic strip are made visible in a transmission polariscope (see Fig. 1) as the strain wave propagates down the length of the core sample.

The birefringent-strip method for determining attenuation coefficients, as well as defining the general characteristics of strain-wave propagation in rock rods has several advantages over the use of strain gages as employed by Goldsmith.[4] The birefringent-strip method provides data along the entire length of the rod vs. data at a few points along the core from strain gages. For this reason, the influence of heterogeneities and fault lines in the core can be observed and separated from attenuation effects.

Daniel and Rowlands[5] have also investigated attenuation in rock samples. They studied, in particular, the behavior of Vermont marble and Cold Spring granite, utilizing photoelastic coatings and moiré techniques.

A more-detailed explanation of the birefringent-strip technique as utilized in this investigation is given by Frasier and Robinson.[2,3]

Experimental Procedure

The physical properties of Charcoal granite, Salem limestone and Berea sandstone as determined by Hjelmstad[6] *et al* and Fischer[7] are presented in Table 1. The rods utilized were core samples 1 in. (25 mm) in diameter, 18 in. (0.46 mm) in length and were obtained from the U.S. Bureau of Mines. A polycarbonate strip 1/8 in. (3.2 mm) thick by 6 in. (150 mm) wide and 17 in. (400 mm) long was bonded to the rock rods as is shown in Fig. 2. The polycarbonate strip is marketed by Photolastic Inc. under the trade name of PSM-1 and was optically stress free. A quick-curing epoxy cement was used to bond the sheet to the rod.

W. L. Fourney, J. W. Dally and D. C. Holloway are Professor, Professor and Associate Professor, respectively, Dept. of Mechanical Engineering, University of Maryland, College Park, MD.

Paper was presented at 1975 SESA Spring Meeting held in Chicago, IL on May 11-16.

Original manuscript submitted: August 4, 1974. Revised version received: November 10, 1975.

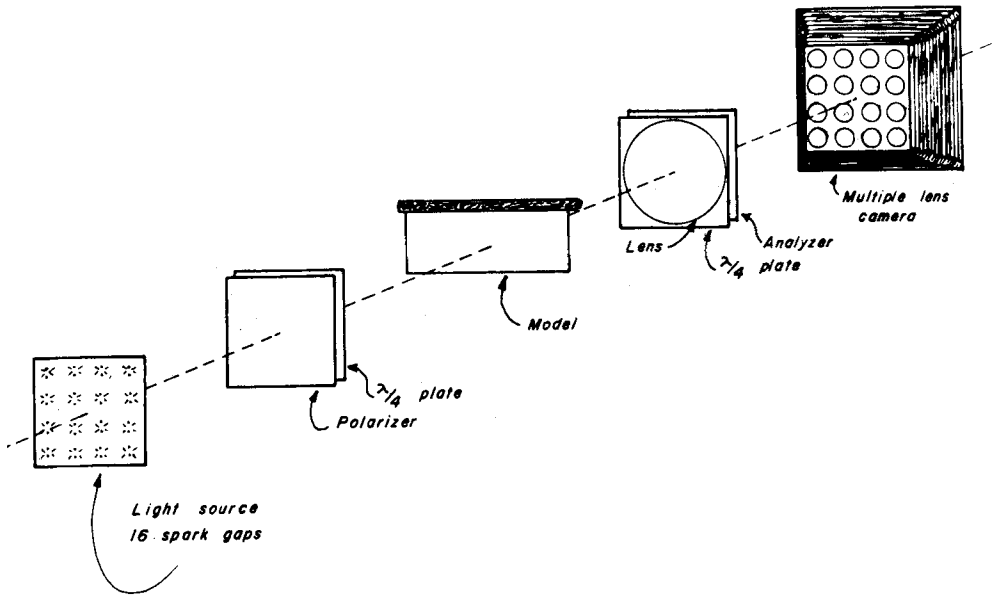

Fig. 1—Rock core with a birefringent strip in a dynamic photoelastic transmission polariscope

The rod–strip combination was supported by thin wires attached to each end of the rod and dynamically loaded by detonating a 560-mg charge of lead azide which was attached to one end of the rod. The lead azide was detonated with a 2000-V 20-joule firing pulse.

The propagating stress waves in the polycarbonate strip were photographed in a light-field dynamic polariscope which consisted of two sheets of circular Polaroid HNCP-37 commercially available from the Polaroid Corp. A multiple-spark-gap camera was used to record the resulting dynamic isochromatic-fringe patterns. This camera was described in detail previously by Riley and Dally[8] and only a summary description will be reported here. The camera is capable of 16 frames and can be operated at framing rates which can be varied in discrete steps from 30,000 to 800,000 fps. The dyamic resolution of the camera is a function of fringe gradient and fringe velocity. Experiments indicate that gradients of 0.8 fringes/mm with fringe velocities of 3,000 m/s represent the upper limit of the resolution capability.

Experimental Results

Typical photoelastic results showing stress-wave propagation in Salem limestone are presented in Fig. 3 where three frames of a 16-frame sequence of records are shown. The first frame in Fig. 3 was taken 60 μs after detonating the charge on the right hand end of the core. The leading stress wave in the birefringent strip, a dilatational (P) wave, makes an angle of 22.5 deg with the rod and exhibits a peak fringe order of 3.5 fringes. The trailing stress wave is a shear or S type which makes an angle of 11.8 deg with the core.

Both wavefronts are plane over most of their length and these angles of inclination of the wavefronts relative to the rod remain constant. Examination of the fringe patterns for Frames 5 and 8 in Fig. 3 show

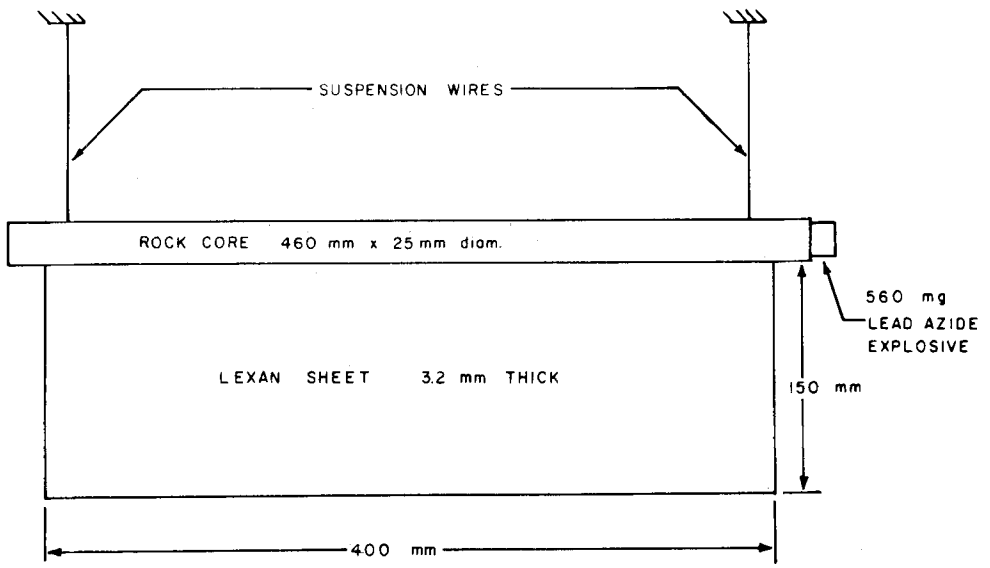

Fig. 2—Geometry of rock cores and birefringent strip

TABLE 1—PROPERTIES OF THREE TYPES OF ROCK

Rock Type	Dynamic Modulus $E \times 10^6$ psi	Poisson's Ratio ν —	Density w(lb/in.^{3})	Tensile Strength (psi)	Compressive Strength (psi)	Rod-Wave Velocity V_R(in./s)
Salem Limestone	5.5	.27	0.0846	760	6,400	159,000
Charcoal Granite	7.8-9.5	.32	0.0985	1800	28,400	175,000
Berea Sandstone	1.23	.33	0.0765	155	6,700	79,000
	GPa	—	g/cc	MPa	MPa	m/sec
Salem Limestone	37.9	.27	2.34	5.23	44	4030
Charcoal Granite	53.8-65.5	.32	2.72	12.4	196	4450
Berea Sandstone	8.5	.33	2.11	1.07	46	2010

more clearly the fringe order along the wavefronts. For instance, in Frame 8, it is evident that the maximum fringe order along the front of the P wave decays from 2.5 to 1.0 fringes and along the front of the S wave from 7.5 to 5.5 fringes. It should be noted that measurements of the strains over a length of 12-rod diameters are possible on each of the first 11 frames taken in this sequence of high-speed photographs. Data from Frames 12 to 16 were disregarded since they were obscured by effects of the reflected stress wave from the free end of the core.

Similar results for the dynamic photoelastic-fringe patterns associated with the Charcoal-granite rod are presented in Fig. 4. In this experiment, the amplitude of the stress wave propagating down the bar was reduced by venting the explosive charge and, as a consequence, the stress waves are of lower amplitude. The P wave makes an angle of 19.4 deg with the rod and the shear wave makes an angle of 10.8 deg with the rod. As was the case for the results with Salem limestone, these wavefronts are straight and the angles of inclination remain essentially constant as the strain pulse propagates down the length of the core. Due primarily to the lower-level loading, the P wave exhibits a maximum fringe order of 0.5 and the shear wave a maximum fringe order of 2.5.

The final experiment in this series of three was conducted with Berea sandstone, and representative results from the photoelastic test are shown in Fig. 5. Inspection of the fringe patterns show that the wavefronts for both the P and S wave are not plane. The curvature indicates that the velocity of the strain wave in the Berea sandstone is decreasing with the distance travelled. It is also important to note the very significant attenuation in the maximum fringe orders associated with the P and S wave as the bar wave propagates along the length of the core. The angle of the P wavefront at the rod-strip interface varies from 55 deg in the earliest frame to 61.6 deg

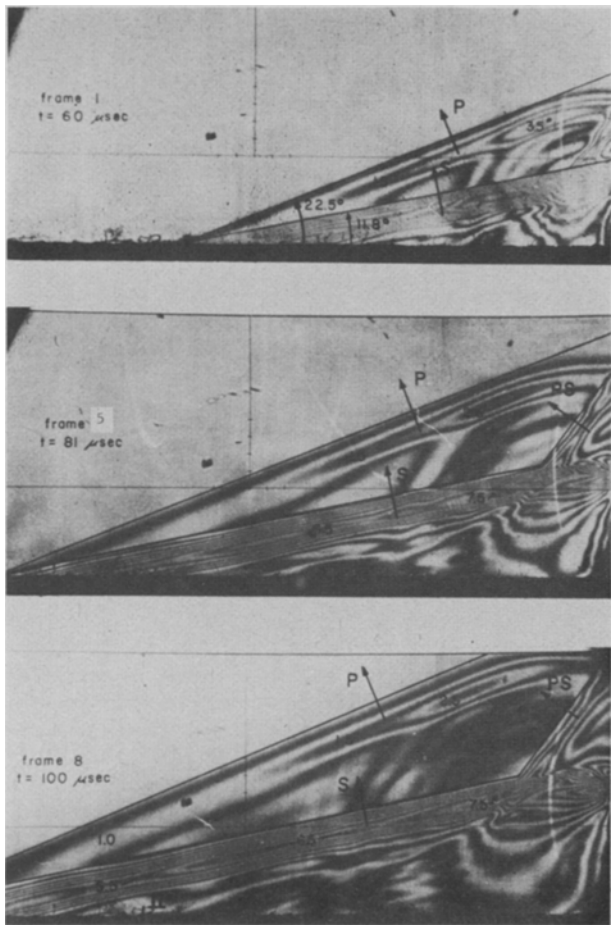

Fig. 3—Dynamic isochromatic-fringe pattern for strain-wave propagation in Salem limestone

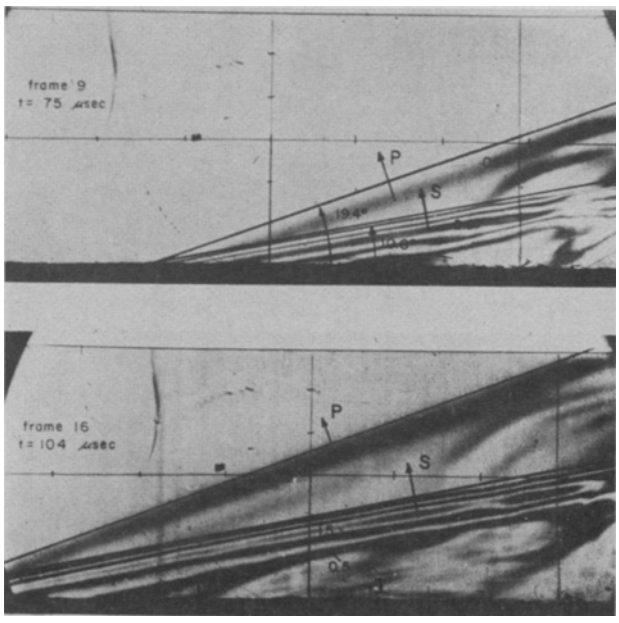

Fig. 4—Dynamic isochromatic-fringe pattern for strain-wave propagation in Charcoal granite

after the wave has propagated 200 mm down the rod. Similarly, the inclination angle for the S wavefront varies from 27 to 30 deg over the same time interval.

Data Analysis

There are two sources of energy loss as the strain wave propagates down the rock core. The birefringent strip that is bonded to the rod removes energy from the core as it is deformed by the passage of the strain wave. In addition, there is another loss of energy in the rock material due to internal friction, local inelastic deformation, microfractures, etc. It is this latter energy loss that is to be determined, for it is an indication of the ability of the type of rock to transmit vibrational disturbances from blast sites to adjacent structures.

The procedure for estimating the energy loss to the birefringent strip has been established by Frasier and Robinson[2] and is given in Ref. 2 in approximate form as:

$$-\frac{1}{W}\frac{dW}{dx} = \frac{h\,G_p \cos\phi_p}{\pi a^2 E_R \cos(\phi_p - \phi_s)\sin\phi_s} \qquad (1)$$

where W = total energy in the strain pulse in the bar
dx = an infinitesimal length along the axis of the bar
h = thickness of the birefringent strip
G_p = shear modulus of the strip
a = core radius
E_R = modulus of elasticity of the rod
ϕ_p and ϕ_s = angle between the P and S wavefronts and the rod respectively

For a given set of test conditions, the right-hand side of eq (1) is a constant C_s and thus

$$-[\log_e W]_{W_1}^{W_2} = [C_s x]_{x_1}^{x_2}$$

or

$$W_2/W_1 = e^{-C_s(x_2 - x_1)} \qquad (2)$$

where it is evident that the constant C_s is the attenuation coefficient associated with the birefringent strip. Substitution of numerical values for the quantities on the right-hand side of eq (1) gives the attenuation coefficients shown in Table 2.

The total energy loss in the bar was determined from the strain-position profiles at two different stations along the length of the bar. The energy contained in the strain pulse at any station is related to the longitudinal strain ϵ in the core according to:

$$W = \frac{1}{2} E_R A \int_l \epsilon^2\,dx \qquad (3)$$

TABLE 2—ATTENUATION COEFFICIENTS FOR 3-MM-THICK POLYCARBONATE STRIPS ON 25-MM ROCK CORES

Type of Rock	C_s (in.$^{-1}$)	C_s ($\times 10^{-3}$ mm^{-1})
Salem Limestone	0.0169	0.665
Charcoal Granite	0.0119	0.470
Berea Sandstone	0.0502	1.980

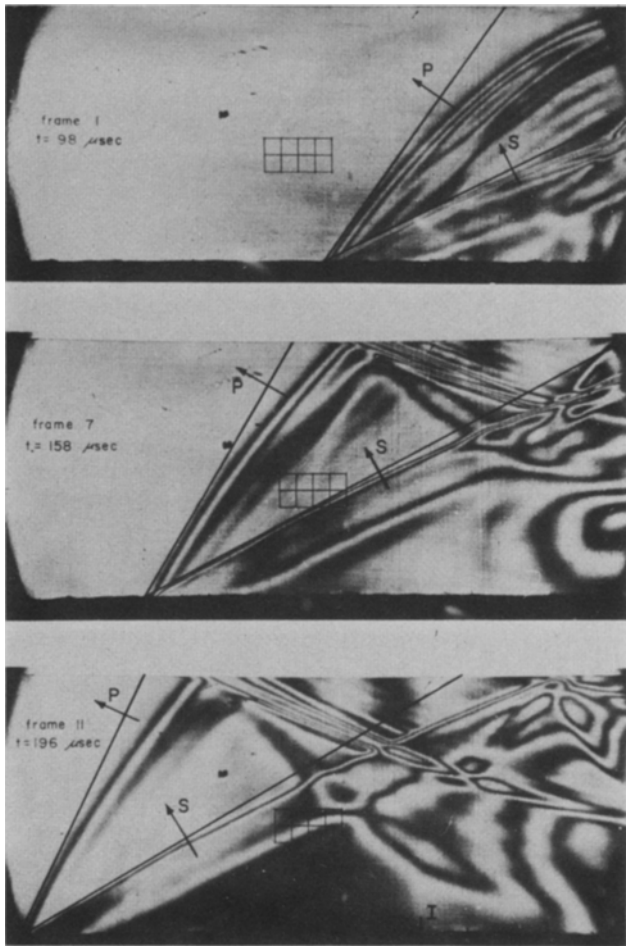

Fig. 5—Dynamic isochromatic-fringe pattern for strain-wave propagation in Berea sandstone

where A is the cross-sectional area of the bar
l is the pulse length of the strain wave

The longitudinal strain in the rock core can be determined from the dynamic isochromatic-fringe pattern from the birefringent strip. If fringe orders associated with the dilatational wave are employed, then:

$$\epsilon = \frac{N_p f_\epsilon}{2h}(1 - \cos 2\phi_p) \qquad (4)$$

and if fringe orders associated with the shear wave are employed, then

$$\epsilon = \frac{N_s f_\epsilon}{2h}\sin 2\phi_s \qquad (5)$$

where f_ϵ is the material-fringe value in terms of strain (1.43×10^{-4} in./fringe or 36.4×10^{-4} mm/fringe, obtained from a static calibration test)
h is the thickness of the birefringent strip

Since the results obtained with the rock cores showed a predominate shear wave, eq (5) was used in the analysis. Substituting this into eq (3) gives:

$$W = B\int_l N_s^2\,dx \qquad (6)$$

where the constant B is given by

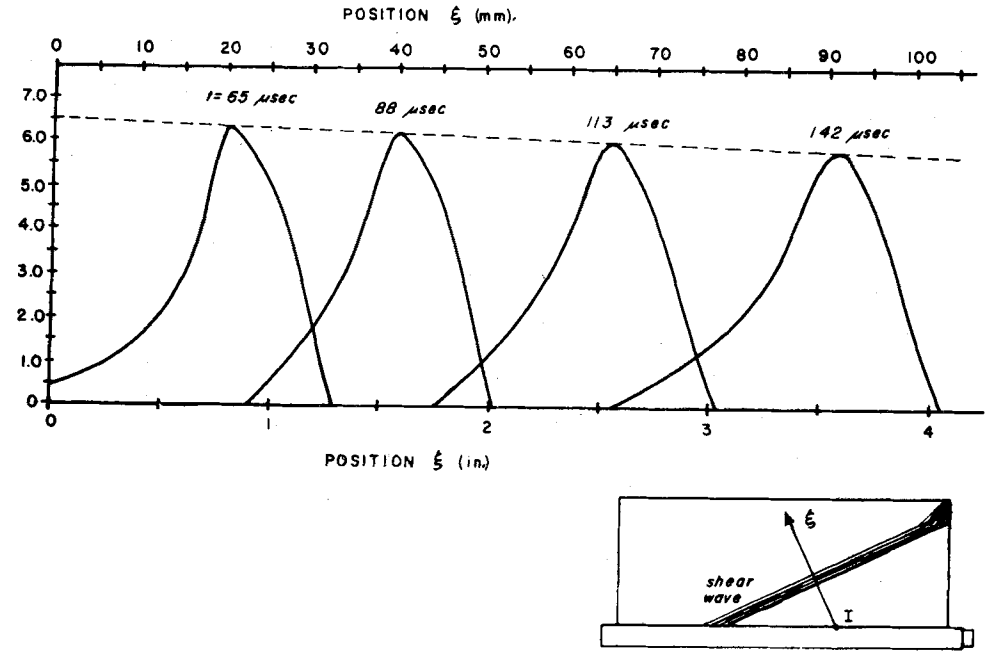

Fig. 6—Fringe-order N_s-position profiles for Salem limestone

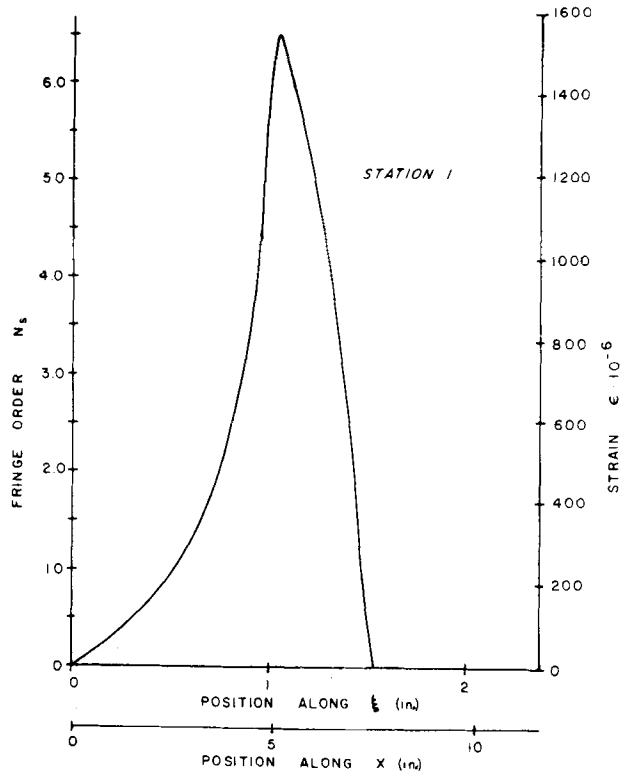

Fig. 7—Strain-position pulse along the Salem-limestone core

$$B = (1/8)E_R A(f_c/h)^2 \sin^2 2\phi_s$$

The value of N_s at the interface between the strip and the core was determined from graphs of the fringe order for the shear wave as a function of position along the wave normal at several different times in the dynamic event. An example of the fringe-order position data for Salem limestone is presented in Fig. 6. Extrapolation of the peak fringe order back to the $\xi = 0$ permitted a correction for the dispersion of the shear wave as it propagated along ξ in the birefringent strip.

The shape of the shear-wave pulse at the interface is then obtained at a specific station as illustrated in Fig. 7 for Salem limestone. This pulse N_s vs. ξ is then converted to a ϵ vs. x pulse by using eq (5) to scale the ordinate and by using

$$x = \xi/\sin\phi_s \qquad (7)$$

to scale the abscissa. This operation was performed at two stations along the length of the rock core. Graphs of N^2 as a function of x were also prepared and numerically integrated to obtain the energy contained in the strain pulses. The results obtained from these calculations are presented in Table 3.

The ratio of the energy at Station 2 to that at Station 1 (W_2/W_1) was substituted into eq (2) to determine the total attenuation coefficient C_T which describes the combined energy loss due to the birefringent strip and the rock. Since the total attenuation coefficient, disregarding second-order terms, is the sum of the attenuation coefficient for the birefringent

TABLE 3—ENERGY IN STRAIN WAVES AT TWO POSITIONS ALONG THE ROCK CORE

Rock Type	W, Energy (in.-lb) Station 1	Station 2	W, Energy (mm-kg) Station 1	Station 2
Salem Limestone*	9.32	7.79	107.5	89.9
Charcoal Granite†	2.10	1.98	24.2	22.8
Berea Sandstone†	.0755	.0433	.872	.050

* Stations 5 in. (127 mm) apart.
† Stations 4 in. (103 mm) apart.

TABLE 4—ATTENUATION COEFFICIENTS C_T AND C_R FOR THREE TYPES OF ROCK

Type of Rock	C_T, (in.$^{-1}$)	($\times 10^{-3}$ mm^{-1})	C_R, (in.$^{-1}$)	($\times 10^{-3}$ mm^{-1})
Salem Limestone	0.0365	1.44	.0196	0.771
Charcoal Granite	0.0143	0.563	.0024	0.0945
Berea Limestone	0.1412	5.56	.0910	3.58

TABLE 5—INCLINATION ANGLE, ROD VELOCITY AND MODULUS OF ELASTICITY FOR THREE TYPES OF ROCK

Type of Rock	ϕ_s, (deg)	V_R, ($\times 10^3$ in./s)	(m/s)	E, ($\times 10^6$ psi)	GPa
Salem Limestone	11.8	202	5130	8.95	61.7
Charcoal Granite	10.8	220	5600	12.3	85.0
Berea Sandstone	27-30	91	1780	1.63	11.2

strip C_s and the attenuation coefficient for the rock alone, C_R, then

$$C_T = C_s + C_R \tag{8}$$

and the energy losses as expressed by C_R due to strain-wave propagation in rock were determined as indicated in Table 4.

The photoelastic data can also be used to determine the rod velocity of the strain wave propagating in the rock core. The angle of inclination of the shear wave relative to the axis of the core is related to the velocity in the rock core V_{Rod} by

$$V_{\text{Rod}} = V_s/\sin\phi_s \tag{9}$$

where V_s is the velocity of the shear wave in the birefringent strip, 41,200 in./s (1050 m/s). Also, the dynamic modulus of elasticity of the rock materials can be determined from the well-known equation for velocity of propagation in a rod:

$$E = (c_s/\sin\phi_s)^2(w/g)$$

where w is the density
g is the gravitational constant

Results obtained for ϕ_s, V_R and E for the three types or rock are summarized in Table 5.

Summary and Conclusions

The birefringent strip bonded to a rock core provides an excellent means to characterize the dynamic properties of rock in a simple and direct fashion. Measurement of the dynamic isochromatic pattern associated with the shear wave in the birefringent strip at two stations along the length of the bar provides sufficient data to determine the bar velocity, the dynamic modulus and the attenuation coefficient.

Since the birefringement strip in effect provides a continuous line of observation along the length of the bar effects of inhomogeneities in the rock core (such as cracks and changes in modulus) can be observed and accounted for in the analysis. Also any viscoelastic effects (such as noted for the Berea sandstone) where the velocities in the rock core vary with the intensity of the strain wave can be observed and the analysis can be extended to account for the nonlinear effects.

The results obtained showed rod velocities and dynamic moduli which were significantly larger than those values reported previously in the literature. These differences may be due to the extremely short loading pulses used to load the bars in this investigation which produced large strain-rate effects.

The accuracy of the results obtained with the birefringent-strip method depends upon what portion of the total energy removed is due to the presence of the strip itself. It is desirable to have the energy removed by the strip [as given by eq (1)] as small as possible. For a given rock sample, therefore, the diameter of the rod should be as large as possible. This increase should also be augmented by using a longer wavelength pulse in order to maintain one-dimensional wave propagation. A decrease in sheet thickness or shear modulus of sheet material would also decrease the energy removed by the strip; however, if the sheet is made too thin, the photoelastic response might become insufficient for accurate reading.

The rock samples used in this study were rather rough with changes occurring in the diameter along the length. More accurate results could be obtained if the rods were centerless ground before the strip was bonded to it.

For the rock types tested, the values of the attenuation coefficients for the Salem limestone and the Berea limestone are more accurate than that obtained for the Charcoal granite. A 10-percent error in C_S for the granite results in a 50-percent error in C_R. This is a large percent error, but even the new value of C_R = .0036/in. is a very small attenuation coefficient. The attenuation coefficient obtained for the granite was lower than that reported by Frasier and Robinson[2,3] for both steel and aluminum.

Acknowledgment

The authors wish to thank the National Science Foundation for its support and encouragement throughout this research program. The efforts of George F. Schilling and Edward G. Freedman in assisting in preparing and conducting the experiments are gratefully acknowledged.

References

1. *Duffy, J. and Lee, T. C., "Measurement of Surface Strain by Means of Bonded Birefringent Strips,"* EXPERIMENTAL MECHANICS, *1 (9), 109-112 (Sept. 1961).*

2. *Frasier, J. T. and Robinson, D. N., "The Measurement of Dynamic Strains Using Birefringent Strips," NSF Research Grant GP 1115/8 Report (May 1964).*

3. *Frasier, J. T. and Robinson, D. N., "The Measurement of Dynamic Strains Using Birefringent Strips," J. of Appl. Mech., 33 (1), 173-181 (March 1966).*

4. *Howe, S. P., Goldsmith, W. and Sockman, J. L., "Macroscopic Static and Dynamic Mechanical Properties of Yule Marble." Paper presented at 3rd SESA International Congress on Experimental Mechanics held in Los Angeles, CA on May 13-18, 1973.*

5. *Daniel, I. M. and Rowlands, R. E., "Wave and Fracture Propagation in Rock Media,"* EXPERIMENTAL MECHANICS, *15 (12), 449-457 (Dec. 1975).*

6. *Krech, W. W., Henderson, F. A. and Hjelmstad, K. E., "A Standard Rock Suite for Rapid Excavation Research," Bureau of Mines RI 7865 (1974).*

7. *Fischer, R., U.S. Bureau of Mines, Twin Cities, Minnesota Private Communication.*

8. *Riley, W. F. and Dally, J. W., "Recording Dynamic Fringe Patterns with a Cranz-Schardin Camera,"* EXPERIMENTAL MECHANICS, *9 (8), 27-33N (1969).*